RSC Advances

PAPER

View Article Online
View Journal | View Issue

Cite this: RSC Adv., 2015, 5, 88382

Synthesis and properties of star-branched nylon 6 with hexafunctional cyclotriphosphazene core†

Chunhua Wang,[ab] Feng Hu,[a] Kejian Yang,[b] Tianhui Hu,[b] Wenzhi Wang,[b] Rusheng Deng,[b] Qibin Jiang[b] and Hailiang Zhang*[a]

Received 4th August 2015
Accepted 9th October 2015

DOI: 10.1039/c5ra15598c

www.rsc.org/advances

A novel star-branched nylon 6 with hexafunctional cyclotriphosphazene core was synthesized using hexa(4-carboxylphenoxy)cyclotriphosphazene (HCPCP) with six carboxyl groups as multifunctional agent in the hydrolytic ring-opening polymerization of ε-caprolactam, and then used for the investigation of mechanical properties, crystallization and rheology behaviors. Star-branching structure and molecular weight have great effects on its properties. Compared with linear nylon 6, star-branched nylon 6 has lower relative viscosity and higher melt flow rate while its mechanical properties can be almost retained by the use of star-branching and an appropriate molecular weight. Research on crystallization behavior indicates that the degree of crystallinity (X_c) of star-branched nylon 6 decreases slightly, but its crystal structure still belongs to α form. The peak crystallization temperature (T_c) and crystallization rate ($1/t_{1/2}$) of star-branched nylon 6 are significantly higher than that of linear nylon 6 because of heterogeneous nucleation induced by HCPCP core, which is beneficial for the use of rapid molding process. As the molecular weight increases, the T_c and $1/t_{1/2}$ of star-branched nylon 6 first increase and then decrease. Capillary rheometer measurement exhibits that the shear viscosity of star-branched nylon 6 decreases with decreasing molecular weight, and the shear viscosity of star-branched nylon 6 with an appropriate molecular weight shows a low value and little or no sensitivity to shear rate and temperature. Such rheology behavior allows for processing at low temperature and low pressure and reduces system cost.

Introduction

Nylon, professionally named polyamide (PA), is a thermoplastics polymer containing amide repeat units on the main chain, which serves as a very important engineering plastic because of excellent properties and wide applications.[1–6] With the rising demand for the precision and appearance of the part, the demand for the processability of nylon material becomes higher. However, traditional nylon is a linear polymer and possesses high viscosity and poor melt flowability, so that it is difficult to be molded into large part with thin wall, precision part or high filler content part. Therefore, developing a new nylon with high flowability has become a hotspot for research.[7–10]

It is well-known that star-branching decreases molecular dimension of polymer and results in a decrease in viscosity and a rise in flowability.[11–13] Theoretically, incorporation of star-branched architecture into nylon molecule can result in some unusual properties compared to linear nylon with similar molecular weight, especially lower viscosity indicating its improved processability, which has been evidenced by Flory's pioneering work on star-branched nylon 6.[7]

Recently, star-branched nylon has attracted increasing interests due to its special properties that set it apart from linear nylon. For example, Fu *et al.* reported the synthesis of star-branched nylon 6 and nylon 12 using trimesic acid and cyclohexanonetetrapropionic acid as tri- and tetra-functional agents and investigation of their viscosities, mechanical properties and crystal morphologies.[14–16] Yuan *et al.* focused on the molecular weights and molecular weight distributions of star-branched nylon 6s obtained by the polymerization of 6-aminocaproic acid in the presence of trimesic acid, EDTA and cyclohexanonetetrapropionic acid as multifunctional agents, and the results showed that the molecular weights calculated were in good agreement with those measured by experiment.[17,18] Zhang *et al.* prepared high-flow nylon 6 with star-branched structure and dendritic polyamidoamine (PAMAM) core by *in situ* polymerization, and its melt flow rate was 70–90% higher than that of linear nylon.[19–21] Wan *et al.* synthesized star-branched nylon 11 using the second generation polypropyleneimine dendrimer (PPI) as multi-functional agent, and investigated its isothermal and nonisothermal crystallization kinetics.[22,23]

Although many studies have been devoted to the synthesis, mechanical property, crystallization behavior, relative viscosity

[a]Key Laboratory of Polymeric Materials & Application Technology, Key Laboratory of Advanced Functional Polymer Materials of Colleges of Hunan Province, College of Chemistry, Xiangtan University, Xiangtan 411105, China. E-mail: zhl1965@xtu.edu.cn

[b]Zhuzhou Times New Material Technology Co. Ltd., Zhuzhou 412007, China

† Electronic supplementary information (ESI) available: HCPCP characterizations and TGA curves of star-branched nylon 6. See DOI: 10.1039/c5ra15598c

and melt flow rate of star-branched nylon, little attention has been paid to the systematic investigation of rheological behavior for star-branched nylon. Research on this aspect is very important because rheological behavior is one of the most important properties for polymer processing and application. Moreover, the multifunctional agents that have been reported and used to synthesize star-branched nylons are limited. Some multifunctional agent reported such as PAMAM is subjected to thermally decompose or undergo a number of side reactions even at a relatively low temperature (~120 °C).[24] For this reason, the corruption and disassociation of PAMAM were doomed to occur when ε-caprolactam and PAMAM were polycondensated at a high temperature (220–260 °C) for a rather long time (>3 h). Undoubtedly, the thermal stability of multifunctional agent is extremely critical for the targeting star-branched nylon to maintain structural integrity during high temperature melting polycondensation process. It is inspiring to find that multifunctional cyclotriphosphazene such as HCPCP can well satisfy this demand because of its excellent thermal stability caused by rigid benzene ring and nitrogen and phosphorus six-member ring structure. Furthermore, HCPCP has simple preparation method, easily controlled process, high yield and low cost. However, to our knowledge, few reports focus on star-branched nylon with multifunctional cyclotriphosphazene core.

In this study, we first chose hexafunctional cyclotriphosphazene HCPCP as multifunctional agent to synthesize a series of star-branched nylon 6 with different molecular weights by the hydrolytic ring-opening polymerization of ε-caprolactam, and then systematically investigated its mechanical properties, thermal properties, crystallization behaviors, flowabilities, and in particular rheological behaviors. Our results will demonstrate how star-branching and molecular weight influence its properties by comparing with linear nylon 6.

Experimental

Materials

Hexachlorocyclotriphosphazene (HCCP, 98%) was purchased from Lanyin Chemical Co., Ltd. 4-Hydroxy benzaldehyde (98%) was purchased from Aladdin. ε-Caprolactam (99%) was provided by Yueyang Chemical Fiber Co., Ltd. All reagents were used as received from commercial sources.

Synthesis of hexa(4-formylphenoxy)cyclotriphosphazene (HAPCP)

4-Hydroxy benzaldehyde (125 g, 1.02 mol), anhydrous K_2CO_3 (140 g, 1.02 mol) and THF (500 mL) were added into a 1 L dried round-bottom flask and stirred at room temperature. Hexachlorocyclotriphosphazene (50 g, 0.14 mol) was dissolved in THF (100 mL) and added dropwise into this flask over 1 h. The reaction mixture was heated to 65 °C and then refluxed for 24 h. The solution was concentrated by rotary evaporation and subsequently precipitated in distilled water. The crude product was washed twice by distilled water. Weight: 114.8 g; yield: 92.8%. The synthetic route of HAPCP is shown in Scheme 1. ^{1}H-NMR (DMSO-d6), δ (ppm): 9.90 (s, 6H, –CHO); 7.76–7.78 (d, 12H, Ar-H), 7.15–7.17 (d, 12H, Ar-H). ^{31}P-NMR (DMSO-d6), δ (ppm): 8.34 (s, 3P, –N=P). Mass Spectrometry (MS) (m/z): $[M + H]^+$ calcd for $C_{42}H_{31}N_3O_{12}P_3$, 862.108; found 862.149.

Synthesis of hexa(4-carboxylphenoxy)cyclotriphosphazene (HCPCP)

HAPCP (50 g, 0.06 mol), NaOH (16 g, 0.40 mol), distilled water (300 mL) and THF (300 mL) were added into a 1 L beaker and stirred at room temperature. $KMnO_4$ (120 g, 0.76 mol) was divided into several parts and added into this beaker in batches until purple red did not fade. After removing the solvent THF, vacuum filtration and acidification, the white solid product, HCPCP was obtained. Weight: 53.7 g; yield: 96.7%. The synthetic route of HCPCP is shown in Scheme 1. ^{1}H-NMR (DMSO-d6), δ (ppm): 12.99 (s, 6H, –COOH); 7.80–7.82 (d, 12H, Ar–H), 6.96–6.98 (d, 12H, Ar–H). ^{31}P-NMR (DMSO-d6), δ (ppm): 8.79 (s, 3P, –N=P). Mass Spectrometry (MS) (m/z): $[M + H]^+$ calcd for $C_{42}H_{31}N_3O_{18}P_3$ 958.077, found 958.257.

Synthesis of star-branched nylon 6

Star-branched nylon 6 was synthesized with reference to the general method for conventional nylon 6,[1] but a multifunctional agent HCPCP with six carboxyl groups was added into this reaction system. A typical procedure is summarized as follows. ε-Caprolactam, HCPCP and distilled water were added into a 5 L autoclave according to the feed compositions as shown in Table 1. The mixture in the autoclave was deoxygenated by repeatedly pumping vacuum and purging with high purity N_2 three times. The reaction system was heated to 250 °C with stirring. The inner pressure reached 0.3–0.8 MPa due to the

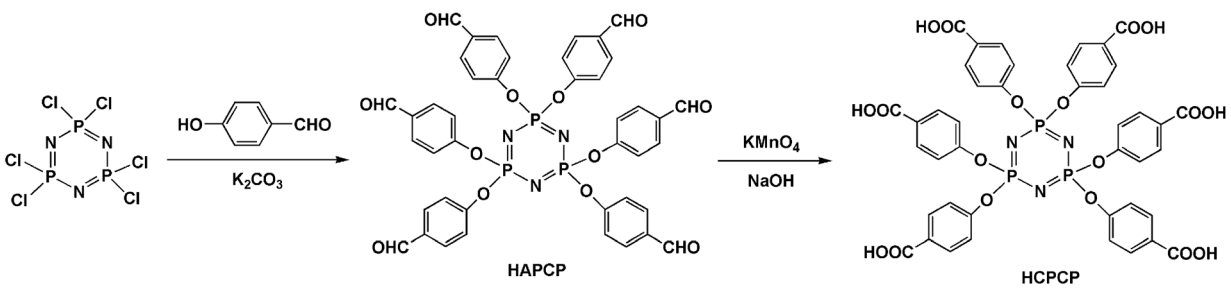

Scheme 1 Synthetic route of HAPCP and HCPCP.

Table 1 Feed compositions of star-branched and linear nylon 6

Sample	Caprolactam (g)	HCPCP (g)	Water (g)
SPA-1	2000	94.1	60
SPA-2	2000	70.6	60
SPA-3	2000	56.5	60
SPA-4	2000	37.6	60
SPA-5	2000	28.2	60
LPA	2000	0	60

spontaneous pressure generated by the water vapor from the reaction system in the autoclave. After heating for 3 h, the inner pressure was gradually reduced to atmospheric pressure about 0.5–1 h. The reaction was then allowed to proceed for a further 2 h at 250 °C under gradually reduced pressure up to −0.07 MPa. Subsequently, the agitator was stopped and the autoclave was filled with N_2. The product was drawn into long strand in water bath and pelletized. These particles were extracted in boiled water for 24 h and then dried under vacuum at 80 °C for 12 h. Five star-branched nylon 6 samples named SPA-1 to SPA-5 were prepared using different concentrations of HCPCP as hexafunctional agent. Linear nylon 6 (LPA) was also prepared using the same preparation process for comparison.

Instrumentation

FTIR spectra were measured with a Nicolet IS 10 Fourier transform infrared spectrometer by the attenuated total reflection (ATR) technology, except HCPCP which was measured by the test mode of KBr pellet. ^{1}H-NMR and ^{31}P-NMR spectra were recorded on a Bruker ARX400 spectrometer at room temperature using deuterated dimethyl sulfoxide (DMSO-d6) or deuterated trifluoroacetic acid (CF_3CO_2D) as the solvent and tetramethylsilane (TMS) as the internal standard. GPC measurements were performed on Agilent 1200 setup equipped with a column set consisting of two PL gel 5 μm MIXED-C columns using trichloromethane as the eluent at 30 °C at a flow rate of 1.0 mL min^{-1}. Narrowly distributed polystyrene standards were utilized for calibration. The samples were dissolved in the mixed solvent of 10% metacresol and 90% trichloromethane before GPC analysis. The weight-average molecular weights ($M_{w,SLS}$) of the samples were assessed by static light scattering (SLS) measurements on a Brookhaven instrument equipped with a 100 mW solid-state laser emitting at 532 nm, a BI-200SM goniometer and a BI-9000 digital correlator scanning from 30° to 120° *via* Zimm extrapolation method.[25,26] BI-DNDC differential refractometer was used to determine the dn/dc of the samples solutions in 90% formic acid containing 1.0 mol L^{-1} potassium chloride. Quantitative determinations of the end groups of –COOH and –NH_2 in the samples were carried out by titration. One gram of each sample was dissolved in 50 mL benzyl alcohol at 150 °C under N_2. The resulting solution was titrated by 0.02 mol L^{-1} KOH solution in methyl alcohol with phenolphthalein as indicator to determine the concentration of –COOH. Similarly, the concentration of –NH_2 was titrated by 0.01 mol L^{-1} HCl solution with bromophenol blue as indicator. The blank titration was carried out at the same time. After titration, the number-average molecular weights ($M_{n,EDT}$) of the samples were calculated according to the reported equation based on Flory model and hypothesis.[14–16]

All the samples for mechanical properties tests were prepared by injection molding. Tensile strength and elongation at break were measured according to GB/T 1040.2-2006. Bending strength and bending modulus were measured according to GB/T 9341-2008. The charpy impact notched strength was measured according to GB/T 1043.1-2008. The moisture contents of the samples were regulated under standard conditions.

Thermal gravimetric analysis (TGA) was carried out on a Mettler Toledo TGA/DSC1 1100SF instrument at a heating rate of 10 °C min^{-1} under N_2. The crystallization and melting behaviors of the samples were detected using DSC 204 F1 differential scanning calorimeter manufactured by Netzsch Company. The temperature and heat flow were calibrated using standard materials (indium and zinc). The scans were performed under N_2 at the heating and cooling rate of 10 °C min^{-1}. The samples with typical mass of 3–10 mg were encapsulated in sealed aluminum pans. The crystal structures of the samples were measured by wide-angle X-ray diffraction (WXRD). The WAXD patterns of melt-crystallized sample films were recorded on a Philips X' Pert Pro diffractometer with a 3 kW ceramic tube as the X-ray source (Cu Kα) and an X' celerator detector in the 2θ range from 3 to 40° at a scanning step of 0.02°.

The relative viscosities of the samples were determined by an Ubbelohde viscometer using 0.01 g mL^{-1} solution in 98% sulfuric acid in 25 °C water bath. The melt flow rates (MFR) in g per 10 min of the samples were measured by a melt flow rate tester (ZRZ1452) made from MTS Company at 235 °C and 0.325 kg load, according to GB/T3682-2000. Rheological behaviors of the samples in melt were investigated by capillary rheometer (RH7-D) made from Malvern Company with shear rates ranging from 50 to 4000 s^{-1}. The capillary diameter (D) was 1.0 mm, its length (L) was 16.0 mm, and the L/D was therefore 16.0. The experiments were carried out at 230, 240, 250 and 260 °C.

Results and discussion

Synthesis of HCPCP

As shown in Scheme 1, a hexafunctional agent HCPCP was successfully synthesized *via* two-step reaction with high yield and low cost. First, HAPCP was synthesized by a nucleophilic substitution reaction between hexachlorocyclotriphosphazene and 4-hydroxy benzaldehyde using anhydrous K_2CO_3 as the deacid reagent. Then, HAPCP was oxidized by $KMnO_4$ to form HCPCP. The chemical structure of HCPCP was confirmed by FTIR (Fig. S1†), ^{1}H-NMR (Fig. 1), ^{31}P-NMR (Fig. S2†) and MS spectrometry (Fig. S3†). Before synthesizing star-branched nylon 6, the thermal stability of HCPCP was examined by TGA at a heating rate of 10 °C min^{-1} from room temperature to 800 °C under N_2. The weight loss curves of HCPCP are shown in Fig. 2. The results indicate that HCPCP has excellent thermal stability with the initial thermal decomposition temperature above 300 °C. Therefore, HCPCP can be used as a multifunctional agent during high-temperature melting polycondensation process of nylon 6.

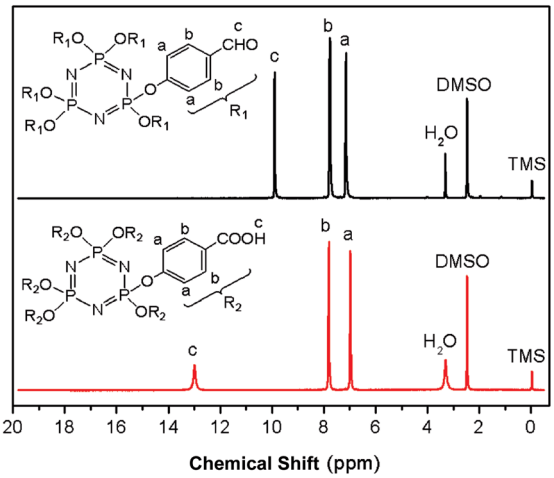

Fig. 1 ^{1}H-NMR spectra of HAPCP and HCPCP in DMSO-d6.

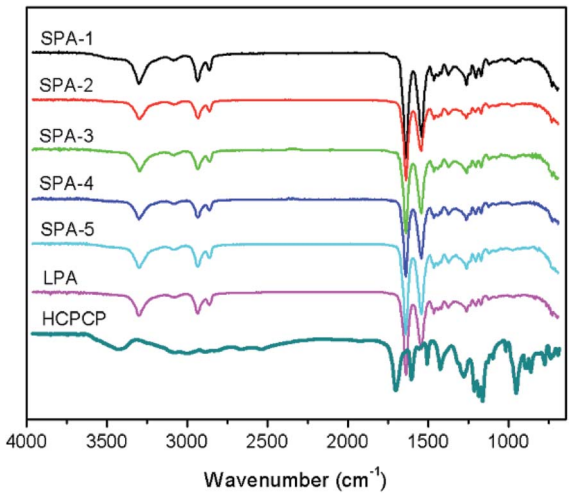

Fig. 3 FTIR spectra of star-branched and linear nylon 6.

Synthesis of star-branched nylon 6

Five star-branched nylon 6 samples with different molecular weights were synthesized using different concentrations of HCPCP as hexafunctional agent in the hydrolytic ring-opening polymerization of ε-caprolactam. The feed compositions of all the samples are listed in Table 1. The chemical structure of star-branched nylon 6 with HCPCP core had been verified by FTIR and ^{1}H-NMR. FTIR spectra of star-branched and linear nylon 6 are shown in Fig. 3. The star-branched nylon 6 exhibits almost the same spectral features as linear nylon 6, such as N–H stretching at 3300 cm^{-1}, C–H stretching 2935 and 2861 cm^{-1}, amide C=O stretching at 1640 cm^{-1}, and N–H and C–N stretching at 1542 cm^{-1}. But under careful observation, the characteristic absorption band of P–O–C of star-branched nylon 6 appears at 960 cm^{-1}, and the intensity of this band increases with increasing concentration of HCPCP in the feed composition. ^{1}H-NMR spectra of star-branched nylon 6 (SPA-3 as a typical example) and linear nylon 6 in CF_3CO_2D are shown in Fig. 4. Compared with linear nylon 6, the characteristic

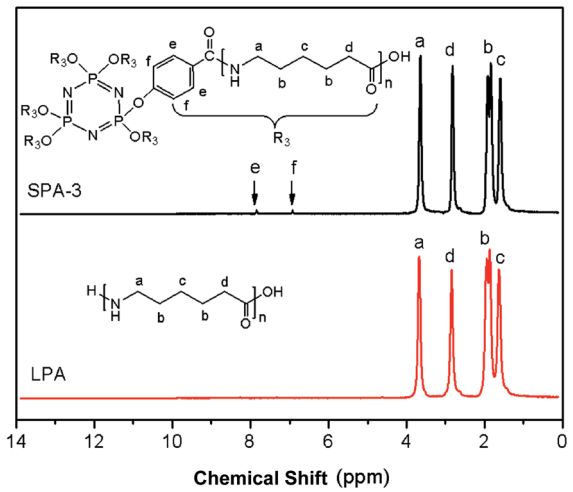

Fig. 4 ^{1}H-NMR spectra of star-branched and linear nylon 6 in CF_3CO_2D.

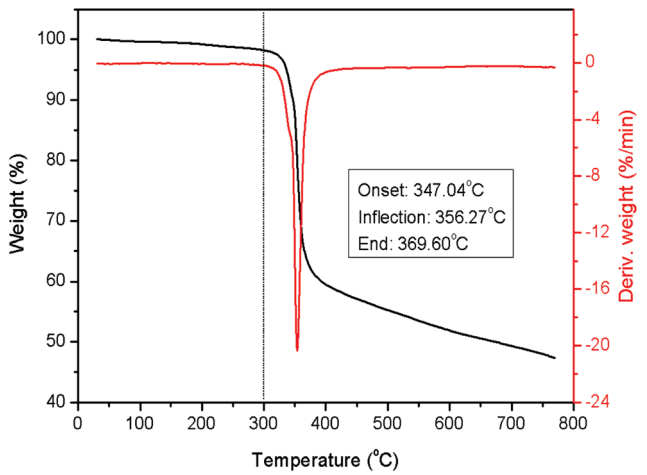

Fig. 2 TGA curves of HCPCP at heating rate of 10 °C min^{-1} under N_2.

resonance peaks of the phenyl of star-branched nylon 6 are presented at 7.80–7.82 and 6.96–6.98 ppm (denoted e and f, respectively). Therefore, these data suggest the existence of star-branched structure.

Molecular weight characterization data of star-branched and linear nylon 6 obtained by end group titration, SLS and GPC are listed in Table 2. As shown in Table 2, the molecular weight obtained by GPC is obviously lower than that obtained by end group titration and SLS due to the smaller hydrodynamic volumes of star-branched nylon 6 in solution. However, all the results indicate that the molecular weight of star-branched nylon 6 mainly depends on the concentration of HCPCP, and the molecular weight increases with decreasing concentration of HCPCP, which are consistent with the results of previous work.[7,17,18] As the concentration of HCPCP decreases to some extent, molecular weight of star-branched nylon 6 can approach and even exceed that of linear nylon 6.

Table 2 Molecular weight characterization data of star-branched and linear nylon 6 obtained by end group titration, SLS and GPC

Sample	$[-COOH]^a \times 10^5$ mol g^{-1}	$[-NH_2]^a \times 10^5$ mol g^{-1}	$M_{n,EDT}{}^a \times 10^{-4}$	$M_{w,SLS}{}^b \times 10^{-4}$	$M_{n,GPC}{}^c \times 10^{-4}$	PDI^c
SPA-1	33.75	3.42	1.18	2.47	0.97	1.98
SPA-2	26.83	2.91	1.45	3.05	1.18	2.03
SPA-3	18.76	2.84	1.82	3.72	1.36	1.87
SPA-4	12.92	2.48	2.37	4.51	1.58	2.10
SPA-5	7.33	2.52	3.01	5.64	1.82	2.28
LPA	5.29	5.47	1.86	3.98	1.67	2.16

[a] The [–COOH] and [–NH_2] values were determined by end group titration, and $M_{n,EDT} = bm/\{[-COOH] + (b-1)[-NH_2]\}$, where m is the sample weight for titration and b is the functionality of multifunctional agent. [b] The $M_{w,SLS}$ was obtained by SLS measurement and Zimm extrapolation method. [c] The $M_{n,GPC}$ and PDI were measured by GPC and calibrated by narrowly distributed polystyrene standards.

Mechanical property

The mechanical properties of injection molded samples of star-branched and linear nylon 6 are shown in Fig. 5. Compared with linear nylon 6, the tensile strength, bending strength, bending modulus and impact strength of star-branched nylon 6 with high molecular weight do not markedly decrease. However, these mechanical properties decrease dramatically when star-branched nylon 6 has low molecular weight, such as SPA-1. The poor mechanical properties of SPA-1 are mainly attributed to its low molecular weight and short arms lengths. Furthermore, the elongation at break of star-branched nylon 6 decreases with decreasing molecular weight, due to the more compact size and the inability to undergo as much reorientation and molecular "slippage".[8] When the molecular weight increases to some extent, the arms lengths become long enough, the mechanical property of star-branched nylon 6 remains at a certain level, approaching that of linear nylon 6.

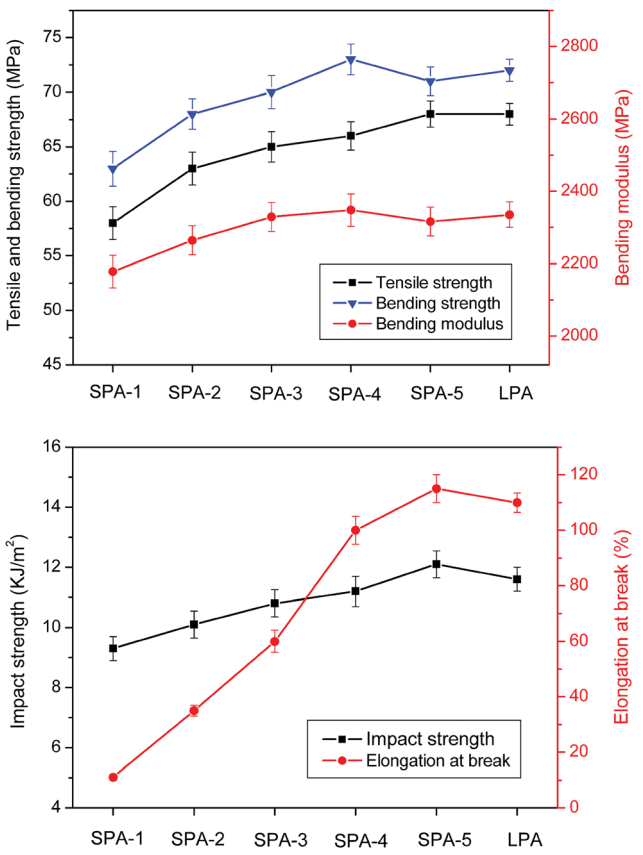

Fig. 5 Mechanical properties of star-branched and linear nylon 6. Error bars represent the standard deviations.

Thermal property and crystallization behavior

The thermal stabilities of star-branched and linear nylon 6 were examined by TGA (Fig. S4†). The results shown in Table 3 indicate that star-branched and linear nylon 6 both have excellent thermal stabilities with the initial thermal decomposition temperatures (T_d) above 380 °C. The crystal structures of star-branched and linear nylon 6 were investigated by WAXD. Fig. 6 shows the WAXD patterns of star-branched and linear nylon 6 after melt-crystallization at 185 °C. The diffraction peaks of star-branched nylon 6 (SPA-3) locate at $2\theta = 20.2$ and 23.4° indexed as 200 and 002/202 reflections, and the crystal structure belongs to α form. It is the same as those of linear nylon 6, indicating that star-branched nylon 6 has the same crystal structure as that of linear nylon 6. Similar results were found for other star-branched nylon 6 samples with different molecular weights as well. Therefore, it can be concluded that star-branching does not change the crystal structure, and HCPCP core is excluded from the crystalline region and located in the amorphous region.

The melting and crystallization behaviors of star-branched and linear nylon 6 were researched by DSC. The DSC thermal diagrams of star-branched and linear nylon 6 during the first cooling and subsequent heating process at a rate of 10 °C min^{-1} are shown in Fig. 7 and the results are listed in Table 3. Note that the melting point (T_m) of star-branched nylon 6 decreases with decreasing molecular weight. The decrease in T_m is ascribed to the rising branched degree and the decreasing hydrogen bond interaction. The degree of crystallinity (X_c) was determined from DSC analysis with the aid of the fusion enthalpy of 230.1 J g^{-1} for the perfectly crystalline nylon 6. As shown in Table 3, the X_c of star-branched nylon 6 is somewhat lower than that of linear nylon 6, since HCPCP core and its adjacent chains are suspected to be unable to crystallize. Scheme 2 shows the schematic illustration of crystallizability and crystallization rate of chains resided at different regions

Table 3 Characteristic parameters for thermal property and melt crystallization of star-branched and linear nylon 6

Sample	T_d[a] (°C)	T_m[b] (°C)	T_c[c] (°C)	ΔH_m[b] (J g^{-1})	X_c[d] (%)	$1/t_{1/2}$[e] (min^{-1})
SPA-1	387.4	217.6	173.8	48.6	21.1	0.77
SPA-2	388.9	218.4	175.6	49.5	21.5	0.86
SPA-3	390.5	219.7	178.3	51.5	22.4	1.01
SPA-4	391.7	219.9	182.5	53.2	23.1	1.38
SPA-5	392.1	220.0	180.1	52.7	22.9	1.23
LPA	392.6	222.1	173.5	53.8	23.4	0.64

[a] The initial thermal decomposition temperature T_d was measured by TGA at a rate of 10 °C min^{-1} under N_2. [b] The melting point T_m and the fusion enthalpy ΔH_m were obtained by DSC during the second heating process. [c] The crystallization temperature T_c was obtained by DSC during the cooling process. [d] $X_c = \Delta H_m/\Delta H_m^0$, $\Delta H_m^0 = 230.1$ J g^{-1}. [e] $1/t_{1/2}$ denotes the crystallization rate and is the reciprocal value of the half-crystallization time when the relative degree of crystallinity (X_t) reaches 50%.

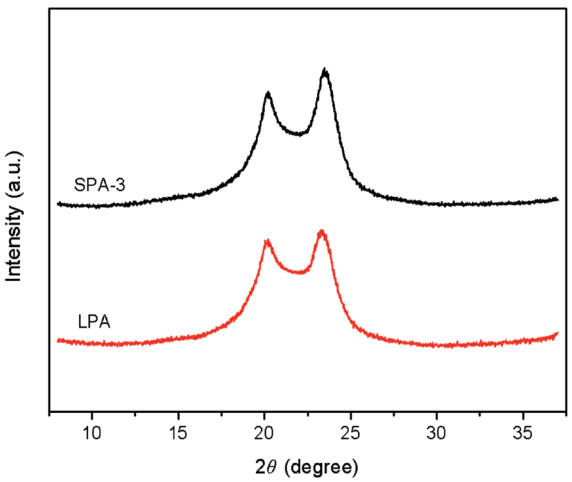

Fig. 6 WAXD patterns of star-branched and linear nylon 6 after melt-crystallization at 185 °C.

depending on the distance to HCPCP core of star-branched nylon 6. The chains of star-branched nylon 6 can crystallize if the free energy change ΔG is less than zero.[27] As the chains are approaching HCPCP core, the crystallization becomes ever harder because of star-branching which restricts the chains folding and increases the free energy to some extent, and meanwhile the crystallization rate becomes ever slower as a result of the chain motion increasingly inhibited by HCPCP core. The X_c of star-branched nylon 6 increases with increasing molecular weight. It is because star-branched nylon 6 with higher molecular weight has less HCPCP core and uncrystallizable chain and therefore is able to form more perfect crystal. With the further increase of the molecular weight, the X_c increases slowly and even reduces slightly due to the more entanglements between the longer arms such as SPA-5.

As shown in Fig. 7, the peak crystallization temperature (T_c) of star-branched nylon 6 is higher than that of linear nylon 6. This result indicates that central HCPCP core can help star-branched nylon 6 to change the manner of nucleation from homogeneous nucleation to heterogeneous nucleation. In other words, HCPCP core plays a more important role than temperature in nucleation and crystallization of star-branched nylon 6. Accordingly, star-branched nylon 6 is easy to nucleate and then crystallize at a higher temperature than linear nylon 6 under the same cooling rate. A similar heterogeneous nucleation phenomenon was also reported in star-branched poly(ε-caprolactone).[28]

Another important parameter for crystallization behavior is the half-crystallization time ($t_{1/2}$), which is the time when

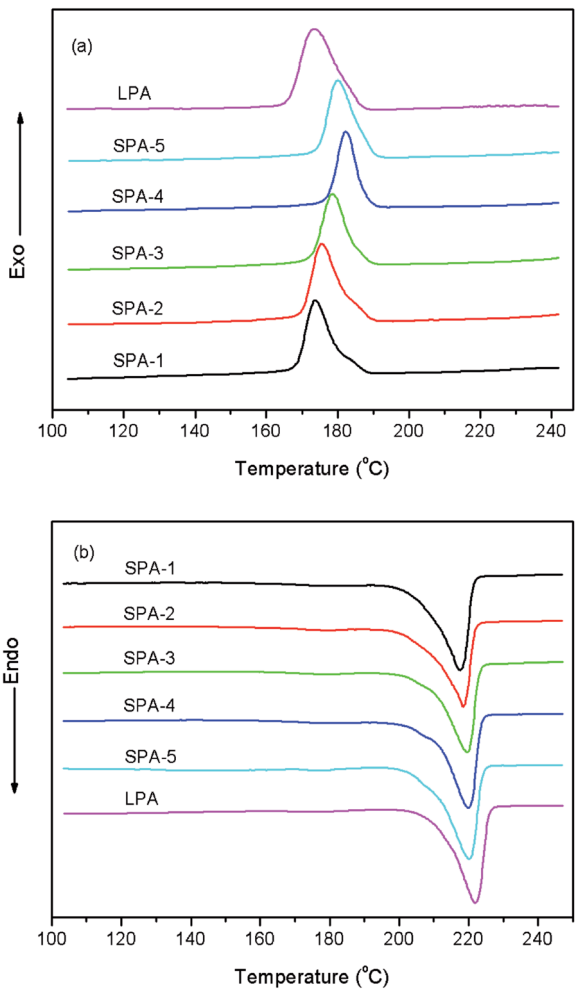

Fig. 7 DSC thermal diagrams of star-branched and linear nylon 6 during the first cooling (a) and the subsequent heating (b) at a rate of 10 °C min^{-1}.

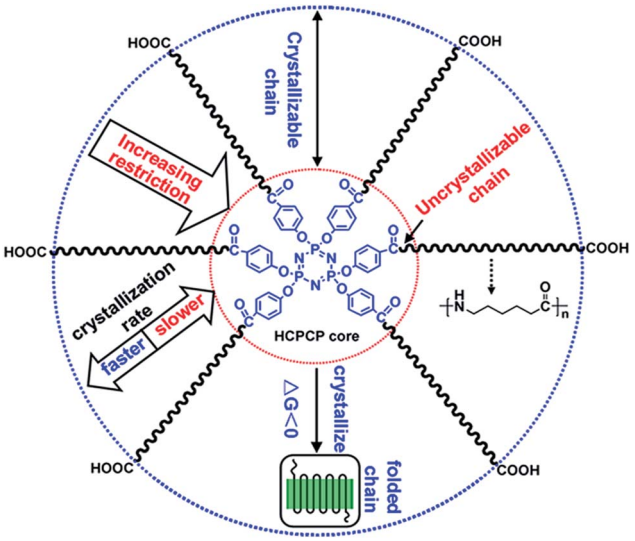

Scheme 2 Schematic illustration of crystallizability and crystallization rate of chains of star-branched nylon 6.

relative crystallinity (X_t) reaches 50%. Its reciprocal value, $1/t_{1/2}$, is often used to represent crystallization rate. Fig. 8 shows the X_t in the course of nonisothermal crystallization for star-branched and linear nylon 6 as a function of crystallization time at a cooling rate of 10 °C min^{-1}. All curves present the similar S-shape, indicating that cooling rate has retardation effect on the crystallization. What's more, the curve of star-branched nylon 6 shifts obviously to the shorter crystallization time region in comparison with linear nylon 6, indicating the faster crystallization rate. The dependence of crystallization rate on the molecular weigh of star-branched nylon 6 is shown in the inset of Fig. 8. With the increasing molecular weight, the $1/t_{1/2}$ of star-branched nylon 6 first increases and then decreases. This may result from the opposite effect of HCPCP core concentration on nucleation rate and crystal growth rate. For SPA-1 to SPA-4 with relatively low molecular weights and high concentrations of HCPCP cores, their crystallization rates depend mainly on crystal growth rates of crystallizable chains. From SPA-1 to SPA-4, the molecular weight increases, the length of crystallizable chain becomes longer, the restriction of HCPCP core on the motion of crystallizable chain decreases, crystal growth rate increases, and thus crystallization rate increases. For SPA-5 with relatively high molecular weight and low concentrations of HCPCP cores, nucleation rate has greater effect on crystallization rate, and nucleation rate decreases obviously due to low concentration of HCPCP core, so its crystallization rate decreases. If the molecular weight continues to increase, we can infer by theoretically that the crystallization rate of star-branched nylon 6 will further decrease and approach that of linear nylon 6. Molecular weight effect on crystallization behavior of star-branched nylon 6 can be also observed from the T_c values listed in Table 3. The effect of molecular weight on T_c is similar to that of $1/t_{1/2}$. For star-branched nylon 6, the fast crystallization rate will contribute to the use of rapid molding process.

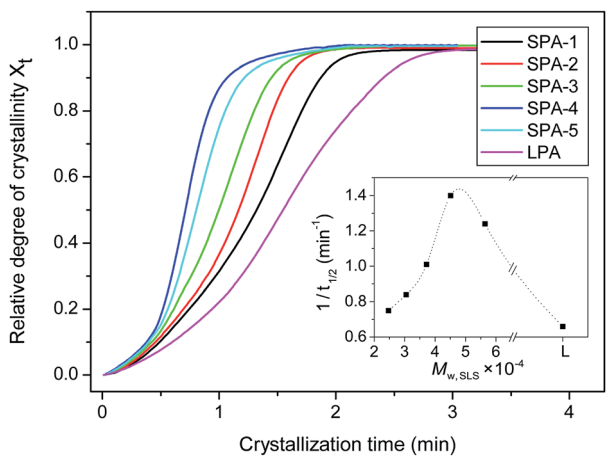

Fig. 8 Relative crystallinity (X_t) of star-branched and linear nylon 6 as a function of crystallization time. The inset shows the dependence of crystallization rate $1/t_{1/2}$ on the molecular weigh of star-branched nylon 6.

Flow property and rheological behavior

Usually, relative viscosity (RV) and melt flow rate (MFR) are used to rapidly evaluate the flow property of thermoplastic polymer. Fig. 9 shows the results of RV and MFR of star-branched and linear nylon 6. As shown in Fig. 9, the RV of star-branched nylon 6 decreases markedly with decreasing molecular weight, and the RV of star-branched nylon 6 is significantly lower than that of linear nylon 6 except SPA-5. This decrease in RV of star-branched nylon 6 is attributed to the smaller hydrodynamic volume and less entanglement between arms, which was also reported by previous researchers.[7,8,14–19] The RV of SPA-5 is slightly higher than that of linear nylon 6, because of its longer arms lengths and more entanglements between the longer arms. Similar flow property is also confirmed by the result of MFR. When the molecular weight decreases, the MFR of star-branched nylon 6 dramatically increases. The MFR of SPA-1 is about six times higher than that of linear nylon 6, and the MFR of SPA-5 is slightly lower than that of linear nylon 6. All of these

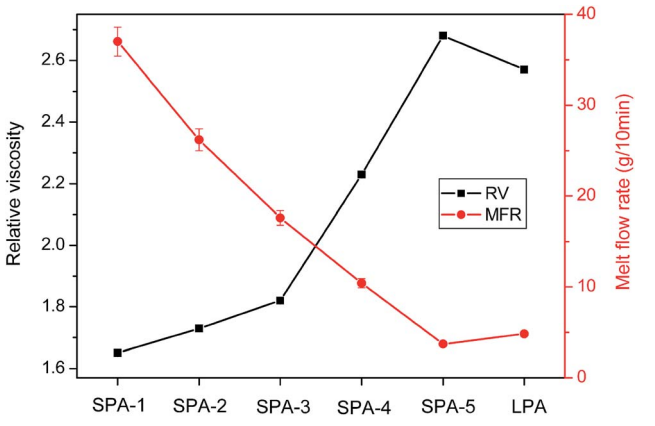

Fig. 9 Relative viscosity and melt flow rate of star-branched and linear nylon 6. Error bars represent the standard deviations.

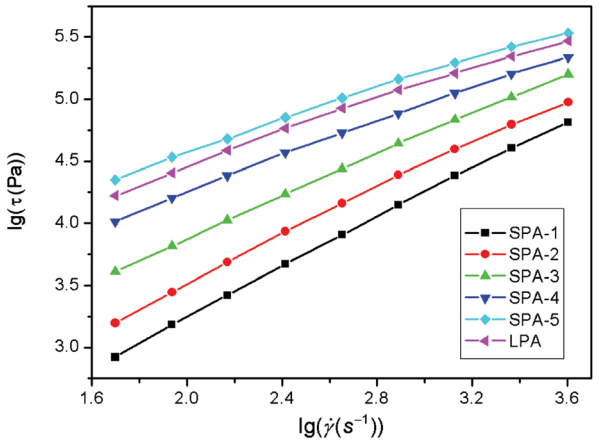

Fig. 10 Rheological curves of star-branched and linear nylon 6 at 230 °C.

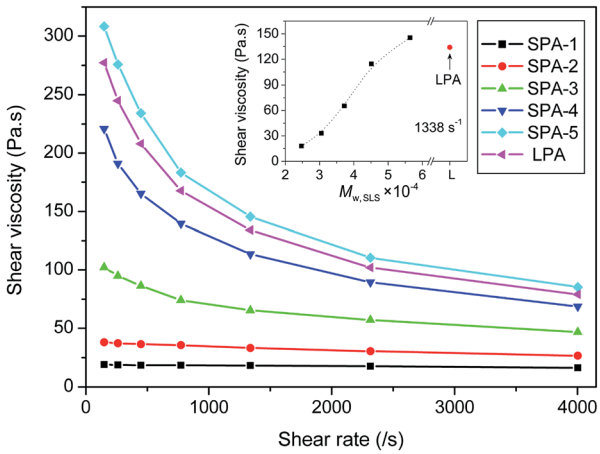

Fig. 11 Shear rate dependence of shear viscosity of star-branched and linear nylon 6 at 230 °C. The inset shows the dependence of shear viscosity on the molecular weigh of star-branched nylon 6.

results indicate that star-branched nylon 6 with relatively low molecular weight has better flow property than linear nylon 6, and star-branching has a stronger effect on melt viscosity than dilute solution viscosity.

To systematically investigate rheological behaviors of star-branched and linear nylon 6, capillary rheometry was applied. Fig. 10 shows the rheological curves of star-branched and linear nylon 6 at 230 °C. As shown in Fig. 10, shear stress increases with the increasing shear rate, but the relationship between shear stress and shear rate is nonlinear. Therefore, the melts of star-branched and linear nylon 6 exhibit non-Newtonian rheological behaviors.

Non-Newtonian index (n) is usually used to represent the degree of deviation from Newtonian fluid. The linear least square method is applied to fit lg τ *vs.* lg γ curve, and the slope of the fitting straight line is the n value. Table 4 lists the n values of star-branched and linear nylon 6 at different temperatures. All the n values are less than 1.0, which further indicates the melts of star-branched and linear nylon 6 are pseudoplastic fluids. The value of n essentially reflects the sensitivity of shear viscosity to shear stress and shear rate. At the same temperature, the n value of star-branched nylon 6 reduces with increasing molecular weight, which means the degree of deviation from Newtonian fluid increases accordingly, due to the more entanglements between the longer arms. Compared with linear nylon 6, the n value of star-branched nylon 6 with relatively low molecular weight is higher and approaches 1.0, so the shear viscosity of star-branched nylon 6 with relatively low molecular weight is not sensitive to shear stress and shear rate. Moreover, the n value of star-branched and linear nylon 6 increases with the rise of temperature. This result demonstrates that the sensitivity of shear viscosity to shear stress and shear rate weakens with the rising of temperature.

Table 4 Non-Newtonian indexes of star-branched and linear nylon 6 at different temperatures

	Non-Newtonian index (n)					
T (°C)	SPA-1	SPA-2	SPA-3	SPA-4	SPA-5	LPA
230	0.92	0.90	0.83	0.70	0.61	0.63
240	0.95	0.93	0.87	0.76	0.67	0.68
250	0.97	0.95	0.90	0.81	0.76	0.75
260	0.98	0.97	0.92	0.85	0.80	0.78

Fig. 11 shows the dependence of shear viscosity of star-branched and linear nylon 6 on shear rate at 230 °C. The shear viscosity of star-branched and linear nylon 6 reduces with increasing shear rate, exhibiting a shear thinning behavior of pseudoplastic fluid. This is because molecular chains orient along the flow direction and disentangle at high shear rate, and the relative motions between molecules become easier. Compared with linear nylon 6, the shear viscosity of star-branched nylon 6 with relatively low molecular weight shows a low value and little or no sensitivity to shear rate, which agree well with the result of n. The dependence of shear viscosity on the molecular weigh of star-branched nylon 6 is shown in the inset of Fig. 11. The shear viscosity of star-branched nylon 6 increases with increasing molecular weight, due to the longer arms lengths and the more entanglements between the longer arms. When the molecular weight increases to some extent, the shear viscosity of star-branched nylon 6 can reach and even exceed that of linear nylon 6. This result is consistent with the aforementioned result of relative viscosity.

Fig. 12 shows the temperature dependence of shear viscosity of star-branched and linear nylon 6 with shear rate at 1338 s^{-1}. The shear viscosity reduces with increasing temperature. As the temperature increases, the movement of chain segment increases, the free volume of the melt increases, intermolecular interaction weakens, and thus shear viscosity reduces. Flow activation energy (ΔE_η) reflects the sensitivity of shear viscosity to temperature. At the constant shear rate, the relationship between shear viscosity and temperature follows Arrhenius equation, so the ΔE_η value can be calculated by the slope of lg η *vs.* T^{-1} straight line. The ΔE_η values of star-branched and linear nylon 6 at different shear rates are listed in Table 5. As shown in

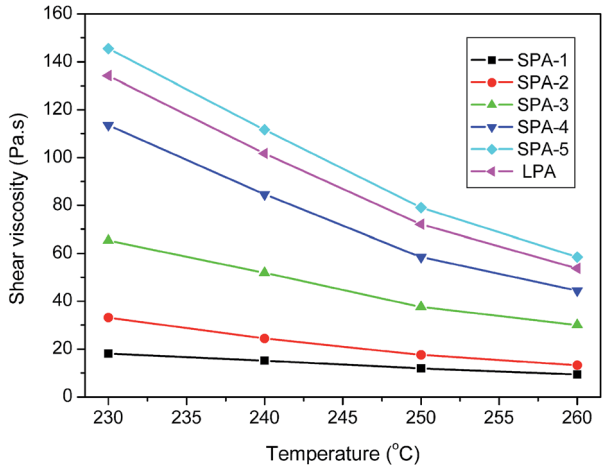

Fig. 12 Temperature dependence of shear viscosity of star-branched and linear nylon 6 with shear rate at 1338 s^{-1}.

Table 5 Flow activation energies of star-branched and linear nylon 6 at different shear rates

	ΔE_η (kJ mol^{-1})					
γ (s^{-1})	SPA-1	SPA-2	SPA-3	SPA-4	SPA-5	LPA
259	58.03	64.29	68.32	73.52	75.65	73.74
1338	53.22	58.45	64.07	68.28	71.80	70.25
2314	50.56	54.76	61.28	65.16	67.26	67.76
4000	48.14	52.03	58.65	62.39	64.42	65.18

Table 5, with the increase of shear rate, the ΔE_η value decreases, that is to say the sensitivity of shear viscosity to temperature weakens. The increase of shear rate is benefit to disentanglement and the number of entanglement points decreases accordingly, so the ΔE_η value decreases. At the same shear rate, the ΔE_η value of star-branched nylon 6 increases with increasing molecular weight, due to the more entanglement between long arms. This phenomenon can be also observed in Fig. 12. Compared with linear nylon 6, star-branched nylon 6 with relatively low molecular weight shows a lower ΔE_η value, so its shear viscosity is not sensitive to temperature as well. Such rheological behavior allows star-branched nylon 6 with appropriate molecular weight to process at low temperature and low pressure and reduces system cost. When the molecular weight increases to some extent, the ΔE_η value of star-branched nylon 6 is no longer strongly dependent on the molecular weight and approaches that of linear nylon 6.

Conclusion

In this study, a new approach was applied for synthesizing star-branched nylon 6 using HCPCP as multifunctional agent in the hydrolytic ring-opening polymerization of ε-caprolactam. The chemical structure of star-branched nylon 6 was verified by FTIR and ^{1}H-NMR. The molecular weight and molecular weight distribution were determined by end group titration, SLS and GPC, and the molecular weight reduces when the concentration of HCPCP increases. Compared with linear nylon 6, the viscosity of star-branched nylon 6 significantly decreases, but its mechanical properties are almost retained by the use of star-branching and an appropriate molecular weight. The crystal structure of star-branched nylon 6 was researched by WAXD. Star-branching does not change the crystal structure and the crystal structure of star-branched nylon 6 still belongs to α form. The crystallization and melting behaviors of star-branched nylon 6 were investigated by DSC. The melting point (T_m) and the degree of crystallinity (X_c) of star-branched nylon 6 decrease slightly due to less perfect crystal caused by branching. However, the peak crystallization temperature (T_c) and the crystallization rate ($1/t_{1/2}$) of star-branched nylon 6 are obviously higher than that of linear nylon 6 on account of heterogeneous nucleation induced by HCPCP core. Moreover, the T_c and $1/t_{1/2}$ of star-branched nylon 6 first increase and then decrease with increasing molecular weight resulting from the opposite effect of HCPCP core concentration on nucleation rate and crystal growth rate. The rheological behavior was investigated by capillary rheometer. As the molecular weight decreases, the shear viscosity of star-branched nylon 6 decreases. The shear viscosity of star-branched nylon 6 with appropriate molecular weight shows a low value and little or no sensitivity to shear rate and temperature. Such star-branched nylon 6 as an easy processing nylon resin offers higher flowability, faster crystallization rate and lower processing temperature and pressure with no significant effect on mechanical properties compared to traditional linear nylon 6, and the prospect of application will be bright. Further studies on this new star-branched nylon 6 with HCPCP core are in progress, such as flame retardant property, industrial research, functional application and so on.

Acknowledgements

This research was financially supported by the National Science & technology Support Plan Project of China (2013BAE02B03) and the Special Fund for the development of Strategic Emerging Industry of China.

Notes and references

1 M. E. Rogers and T. E. Long, *Synthetic methods in step-growth polymers*, John Wiley & Sons, New York, 2003.
2 J. E. Mark, *Polymer data handbook*, Oxford University Press, Oxford, 1999.
3 K. Shi, L. Ye and G. Li, *RSC Adv.*, 2015, **5**, 30160–30169.
4 G. Zhang, Y. X. Zhou, Y. Kong, Z. M. Li, S. R. Long and J. Yang, *RSC Adv.*, 2014, **4**, 63006–63015.
5 M. Shabanian, N. J. Kang, J. W. Liu, U. Wagenknecht, G. Heinrich and D. Y. Wang, *RSC Adv.*, 2014, **4**, 23420–23427.
6 M. Shabanian, N. J. Kang, D. Y. Wang, U. Wagenknecht and G. Heinrich, *RSC Adv.*, 2013, **3**, 20738–20745.
7 J. R. Schaefgen and P. J. Flory, *J. Am. Chem. Soc.*, 1948, **70**, 2709–2718.
8 J. M. Warakomski, *Chem. Mater.*, 1992, **4**, 1000–1004.
9 B. N. Epstein and W. Del, US Pat., US5274033 A, 1993.

10 N. Hasegawa, A. Usuki, A. Okada and T. Kurauchi, US Pat., US5346984A, 1994.
11 W. Burchard, *Adv. Polym. Sci.*, 1999, **143**, 113–194.
12 T. C. B. Mcleish and S. T. Milner, *Adv. Polym. Sci.*, 1999, **143**, 195–256.
13 H. A. Klok, S. Becker, F. Schuch, T. Pakula and K. mullen, *Macromol. Chem. Phys.*, 2002, **203**, 1106–1113.
14 P. Fu, M. L. Wang, M. Y. Liu, Q. Q. Jing, Y. Cai, Y. D. Wang and Q. X. Zhao, *J. Polym. Res.*, 2011, **18**, 651–657.
15 P. Fu, Q. Q. Jing, M. Y. Liu, S. H. Yang, Y. D. Wang and Q. X. Zhao, *Polym. Mater. Sci. Eng.*, 2011, **27**, 33–35.
16 P. Fu, Q. Q. Jing, M. Y. Liu, Y. D. Wang, S. H. Yang, M. L. Wang and Q. X. Zhao, *Polym. Mater. Sci. Eng.*, 2011, **27**, 46–49.
17 C. M. Yuan, G. D. Silvestro, F. Speroni, C. Guaita and H. C. Zhang, *Macromol. Chem. Phys.*, 2001, **202**, 2086–2092.
18 C. M. Yuan, G. D. Silvestro, F. Speroni, C. Guaita and H. C. Zhang, *Macromol. Symp.*, 2003, **199**, 109–124.
19 F. Zhang, L. Zhou, Y. C. Liu, W. J. Xu and Y. Q. Xiong, *J. Appl. Polym. Sci.*, 2008, **108**, 2365–2372.
20 F. Zhang, L. Zhou, Y. Q. Xiong and W. J. Xu, *J. Polym. Sci., Part B: Polym. Phys.*, 2008, **46**, 2201–2211.
21 F. Zhang, L. Zhou, Y. Q. Xiong, G. P. Liu and W. J. Xu, *J. Appl. Polym. Sci.*, 2009, **111**, 2930–2937.
22 J. T. Wan, Z. Y. Bu, C. Li, H. Fan and B. G. Li, *Thermochim. Acta*, 2011, **524**, 117–127.
23 J. T. Wan, C. Li, H. Fan, Z. Y. Bu and B. G. Li, *Thermochim. Acta*, 2012, **544**, 99–104.
24 D. A. Tomalia, H. Baker, J. Dewld, M. Hall, G. Kallos, S. Martin and J. Roeck, *Polym. J.*, 1985, **17**, 117–132.
25 B. H. Zimm, *J. Chem. Phys.*, 1948, **16**, 1093–1099.
26 P. R. Saunders, *J. Polym. Sci.*, 1962, **57**, 131–139.
27 B. Wunderlich, *Thermochim. Acta*, 2011, **522**, 2–13.
28 W. Y. Xie, N. Jiang and Z. H. Gan, *Macromol. Biosci.*, 2008, **8**, 775–784.